Biochimica et Biophysica Acta 1827 (2013) 1–9

Contents lists available at SciVerse ScienceDirect

Biochimica et Biophysica Acta

journal homepage: www.elsevier.com/locate/bbabio

The fifth electron in the fully reduced caa_3 from *Thermus thermophilus* is competent in proton pumping

Sergey A. Siletsky [a,*], Ilya Belevich [c,1], Tewfik Soulimane [b], Michael I. Verkhovsky [c,2], Mårten Wikström [c]

[a] Department of Molecular Energetics of Microorganisms, A.N. Belozersky Institute of Physico-Chemical Biology, Lomonosov Moscow State University, Moscow, Russian Federation
[b] Chemical and Environmental Science Department and Materials and Surface Science Institute, University of Limerick, Ireland
[c] Helsinki Bioenergetics Group, Institute of Biotechnology, P.O. Box 65, FI-00014, University of Helsinki, Finland

ARTICLE INFO

Article history:
Received 16 August 2012
Received in revised form 21 September 2012
Accepted 24 September 2012
Available online 28 September 2012

Keywords:
Cytochrome *c* oxidase
Charge transfer steps
Catalytic cycle intermediates
Membrane potential
Thermus thermophilus

ABSTRACT

The time-resolved kinetics of membrane potential generation coupled to oxidation of the fully reduced (five-electron) caa_3 cytochrome oxidase from *Thermus thermophilus* by oxygen was studied in a single-turnover regime. In order to calibrate the number of charges that move across the vesicle membrane in the different reaction steps, the reverse electron transfer from heme a_3 to heme *a* and further to the cytochrome c/Cu_A has been resolved upon photodissociation of CO from the mixed valence enzyme in the absence of oxygen. The reverse electron transfer from heme a_3 to heme *a* and further to the cytochrome c/Cu_A pair is resolved as a single transition with $\tau \sim 40$ μs. In the reaction of the fully reduced cytochrome caa_3 with oxygen, the first electrogenic phase ($\tau \sim 30$ μs) is linked to O–O bond cleavage and generation of the $\mathbf{P_R}$ state. The next electrogenic component ($\tau \sim 50$ μs) is associated with the $\mathbf{P_R} \rightarrow \mathbf{F}$ transition and together with the previous reaction step it is coupled to translocation of about two charges across the membrane. The three subsequent electrogenic phases, with time constants of ~0.25 ms, ~1.4 ms and ~4 ms, are linked to the conversion of the binuclear center through the $\mathbf{F} \rightarrow \mathbf{O_H} \rightarrow \mathbf{E_H}$ transitions, and result in additional transfer of four charges through the membrane dielectric. This indicates that the delivery of the fifth electron from heme *c* to the binuclear center is coupled to pumping of an additional proton across the membrane.

1. Introduction

Cytochrome *c* oxidase catalyzes reduction of O_2 to H_2O using electrons supplied by cytochrome *c* from the positively charged side of the membrane. The most thoroughly explored canonical aa_3-type cytochrome *c* oxidases, including enzyme from bovine heart mitochondria [1–7], contain four redox-centers. Two input centers, Cu_A and heme *a*, transfer electrons to the binuclear center (BNC) — the oxygen-reducing site formed by the high-spin iron of heme a_3 and the copper ion of Cu_B, buried in the hydrophobic core of the protein.

Water is formed from oxygen in the BNC and the reaction is coupled to charge separation resulting in net unidirectional transfer of 8 charges across the membrane for each molecule of dioxygen reduced. Half of these charges are generated due to the vectorial nature of the oxygen reduction chemistry itself, since the electrons and protons are taken from opposite sides of the membrane [8]. In addition, cytochrome oxidase uses the energy released during this reaction to pump four additional charges (protons) across the membrane [9]. Despite the well-known three-dimensional structure of several aa_3-type cytochrome oxidases [10–13], the details of the partial electrogenic proton transfer steps during the catalytic cycle are not conclusively established.

The catalytic cycle of cytochrome oxidase can be formally split into "oxidative" and "reductive" halves. Upon reaction of the reduced enzyme with dioxygen the oxidative phase of the catalytic cycle proceeds through several catalytic intermediates ($\mathbf{R} \rightarrow \mathbf{A} \rightarrow \mathbf{P_R} \rightarrow \mathbf{F} \rightarrow \mathbf{O}$), leading to complete four-electron reduction of dioxygen to water and pumping of two protons across the membrane [14–16]. To resolve these steps, the commonly used approach is to study the reaction of the CO-inhibited fully reduced enzyme with molecular oxygen after laser-induced flash photolysis of CO [17]. This approach can be combined with time-resolved spectroscopic or electrometric techniques to identify the stages of electron and coupled proton transfers [4,16,18–24].

In the reductive phase of the catalytic cycle (the $\mathbf{O} \rightarrow \mathbf{E}$ and $\mathbf{E} \rightarrow \mathbf{R}$ transitions) of the aa_3-type cytochrome oxidase, the input of two electrons reduces the binuclear center, enabling the binding of dioxygen to the iron of the high spin heme a_3. The proton transfer events in this part of the reaction cycle are less understood, partly

Abbreviations: BNC, binuclear heme a_3/Cu_B center; HEPES, 4-(2-hydroxyethyl)-1-piperazineethanesulfonic acid; MV-CO, the "mixed valence" state with bound CO; SHE, standard hydrogen electrode; RuAm, hexammineruthenium; TMPD, *N,N,N′,N′*-tetramethyl-1,4-phenylenediamine; τ, time constant; E_m, midpoint redox potential versus SHE; E_h, ambient redox potential versus SHE; DM, (dodecyl L-D-maltoside)

* Corresponding author. Tel.: +7 495 9395549; fax: +7 495 9390338.
E-mail address: siletsky@genebee.msu.su (S.A. Siletsky).
[1] Present address: Electron Microscopy Unit, Institute of Biotechnology, P.O. Box 56, FI-00014, University of Helsinki, Finland.
[2] Deceased 4th October, 2011.

0005-2728/$ – see front matter © 2012 Elsevier B.V. All rights reserved.
http://dx.doi.org/10.1016/j.bbabio.2012.09.013

due to the existence of multiple forms of the oxidized state [15,25]. However it is known that both electron transfer reactions of the reductive phase are coupled to net proton uptake by the protein [26,27]. Also, immediate reduction of the freshly formed $\mathbf{O_H}$ state has been shown to result in electron delivery to the optically invisible Cu_B center, and pumping with a stoichiometry of one proton across the membrane with formation of the one-electron reduced $\mathbf{E_H}$ state [15,28,29]. In the absence of electron donors the $\mathbf{O_H}$ state relaxes into the oxidized ground state (**O**), the reduction of which is not linked to proton pumping [16,30]. However, the structural difference between the **O** and $\mathbf{O_H}$ states is still unclear [28,31].

Cytochrome *caa*$_3$ from *Thermus thermophilus* belongs to the A2 subfamily of the heme–copper oxidases [32–37], but has an additional redox center (heme *c*) covalently linked to its subunit II. Its crystal structure was recently elucidated at 2.3 Å resolution [38]. The presence of five redox centers within the enzyme gives the natural opportunity of time-resolved studies of the re-reduction of the **O** or $\mathbf{O_H}$ state in a single-turnover regime, after oxidation of the fully reduced enzyme by O_2. This reaction otherwise resembles the reaction of the *aa*$_3$-type cytochrome oxidases with O_2, except for the additional reaction that is associated with the delivery of the fifth electron into the BNC [36].

The reaction of cytochrome *caa*$_3$ with dioxygen starts with the binding of O_2 to heme a_3 (compound **A** [39]), which is followed by electron transfer from heme *a* to the BNC with a time constant of about 30 μs, forming the $\mathbf{P_R}$ state [36,40]. In the following step the $\mathbf{P_R}$ state of the binuclear center gives rise to the next compound, the **F** state, with absorption maximum around 580 nm (τ ~ 41 μs). In addition, this transition also includes electron equilibration between the Cu_A/cytochrome *c* pair and heme *a* [36]. Further, the two electrons, equilibrated among the three input redox-centers, heme *a*, Cu_A and cytochrome *c*, are transferred one by one into the BNC during the reduction of compound **F**, converting the BNC via the $\mathbf{O_H}$ state into the final product of the reaction, the $\mathbf{E_H}$ (one-electron reduced) state where Cu_B is the final electron acceptor [36].

In this work, time-resolved electrometry was applied to study the single-turnover oxidation of fully-reduced *caa*$_3$ cytochrome oxidase from *T. thermophilus* by molecular oxygen. The kinetics of membrane potential generation was followed and partial charge transfer events which are coupled to the conversion of the corresponding intermediates of the BNC were determined. In particular, we wished to address the question of whether or not the transition from state $\mathbf{O_H}$ to state $\mathbf{E_H}$, which occurs naturally in this enzyme, is coupled to proton translocation. In order to calibrate precisely the charge transfer steps during the reaction with oxygen, reversed electron transfer ("back-flow") was studied in the absence of dioxygen.

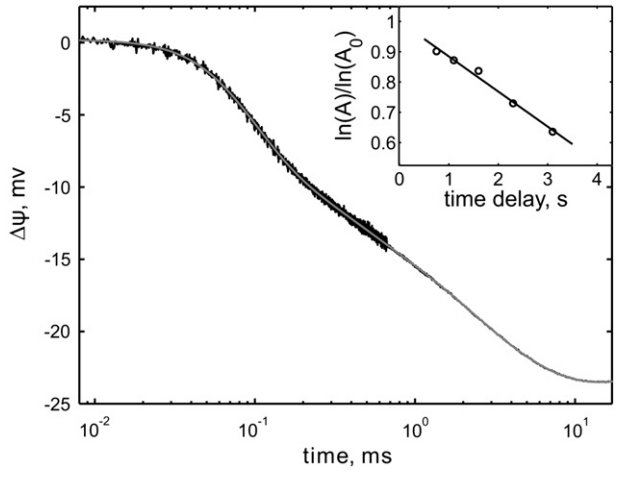

Fig. 1. The kinetics of membrane potential generation during the reaction of fully reduced cytochrome *caa*$_3$ with oxygen (the shown curve is an average of 5 curves). The theoretical fit to the data is shown in gray. The fit gives the following parameters for the model curve: time constants (μs) = [23; 23.4; 50; 250; 1 410; 3 950], amplitudes (mV) = [0; 0.51; 8.09; 4.69; 6.399; 4.76]. The reaction was started at 1.3 s from the beginning of injection of 100 μl of oxygen saturated buffer. Inset: dependence of the amplitude of membrane potential generation during the reaction of fully reduced cytochrome *caa*$_3$ with oxygen on the time delay between oxygen pulse and CO photolysis. The y-coordinate shows the relative amplitudes ln(A)/ln(A0), which are the log of apparent amplitudes normalized to the log of the maximal value of amplitude, obtained from extrapolating the data to τ = 0. Conditions: 100 mM HEPES (pH 7.5), 30 mM glucose, 50 μg/ml catalase, 120 μg/ml glucose oxidase, 3 μM RuAm, 0.67 μM TMPD, 1 mM ascorbate, 100% CO mixture with argon.

2. Material and methods

2.1. Enzyme preparation and reconstitution into phospholipid vesicles

Cytochrome *caa*$_3$ was isolated from *T. thermophilus* HB8 cells as described in [38,41,42]. The enzyme was reconstituted into vesicles by the Bio-Beads method (SM-2 adsorbent; Bio-Rad, Hercules, CA) as described [43], except that the concentration of oxidase during reconstitution was increased to 5–8 μM.

2.2. Time-resolved measurement of electric potential generation

The development of electric potential across the vesicle membrane was monitored by an electrometric technique, as adapted from time-resolved experiments with *aa*$_3$-type cytochrome oxidase. Details of the sample preparation and the methodology can be found in [44].

2.3. Time-resolved spectrophotometric measurements

Time-resolved multi-wavelength absorption changes were followed by a home-constructed CCD-based instrument, which allows recording of surfaces absorption changes with a time resolution of 1 μs between the spectra. This setup has been described in detail [45]. The reaction was initiated by a laser flash (BrilliantB; Quantel, Les Ulis, France; frequency-doubled YAG, 532 nm, pulse energy − 120 mJ).

2.4. Data analysis

The experimental data were fitted by a sequential reaction model [20,44,46]. MATLAB (The Mathworks, South Natick, MA) was used for data analysis and presentation.

3. Results

3.1. Kinetics of membrane potential generation during reaction of the reduced cytochrome *caa*$_3$ from *T. thermophilus* with dioxygen

The flow-flash approach was applied to follow the kinetics of membrane potential generation during reaction of dioxygen with cytochrome *caa*$_3$ incorporated into proteoliposomes. A pulse of oxygen-saturated buffer was given to the fully reduced and CO-inhibited cytochrome *caa*$_3$ in the dark. Shortly (Δτ = 1.3 s) after the start of addition of oxygen-saturated buffer, CO was photodissociated from the BNC by a laser flash to allow oxygen binding. The reaction with oxygen was then monitored by capacitive potentiometry [47].

Fig. 1 shows that the overall pattern of the electrometric response is similar to that obtained earlier for bovine enzyme [20] and cytochrome *ba*$_3$ from *T. thermophilus* [24]. An initial lag phase is followed by five components of membrane potential development, corresponding to transfer of positive charge through the enzyme from the inside to the outside of the liposomes. The lag phase (τ ~ 20–30 μs) is 2–3 times longer than in other heme–copper oxidases [48] and corresponds, by analogy with a previous interpretation [20], to the release of CO, binding of oxygen to heme a_3, and formation of the oxygen adduct, compound **A**.

The second phase of the reaction has a time constant in the range of 23–33 μs, and has the smallest amplitude (maximally ~7% of the total response) of all the phases. The main part of potential generation was formed by the four subsequent components, viz. the third (~50 μs, 28–33%), fourth (~250 μs, ~19%), fifth (~1.4 ms, 26%) and sixth (~4 ms, ~20%) electrogenic phases. The time constant of the third electrogenic component is close to that of the $\mathbf{P_R \rightarrow F}$ transition, determined by optical spectroscopy [36], while the time constants of the fourth and fifth components resemble that of the $\mathbf{F \rightarrow O}$ transition of the aa_3-type oxidases [22,24,49,50].

The observed overall amplitude of the electrogenic response depends strongly on the delay time between addition of dioxygen and the laser flash (Fig. 1, inset). This is due to the relatively fast rate of spontaneous CO dissociation from heme a_3 in the caa_3 enzyme in the dark. As a result, a considerable amount of cytochrome caa_3 reacts with O_2 already before the laser flash. By following the reaction with different time delays (Fig. 1, inset), we determined the rate constant of spontaneous CO dissociation from cytochrome caa_3 as $\sim 0.37 \pm 0.025\ s^{-1}$. Similar values of CO dissociation rates have been observed earlier for caa_3 oxidases from *Bacillus stearothermophilus* ($k_{off} \sim 0.7\ s^{-1}$ [51]) and *Bacillus subtilis* ($k_{off} \sim 0.1\ s^{-1}$ [52]), and for cytochrome ba_3 from *T. thermophilus* ($k_{off} \sim 0.8\ s^{-1}$ [24]). It should be noted that these rates are more than ten times faster than those for cytochrome aa_3 from bovine heart [53]. The rate of spontaneous CO dissociation from heme a_3 makes it possible to estimate the electrogenic response for the entire reactive population of caa_3 enzyme based on

$$A = A_o{}^{*}\exp(-k^{*}t),$$

where A is the experimentally observed amplitude, A_o is the amplitude for the entire enzyme population that reacts with CO, k is the rate constant of spontaneous CO dissociation, and t is the time of delay between O_2 addition and the laser flash. On that basis the total amplitude is estimated to be $\sim 51 \pm 2$ mV.

3.2. Spectroscopic measurements of electron "back-flow" in cytochrome caa_3

The data from the flow-flash experiment do not directly yield the number of charges that move across the vesicle membrane in the different reaction steps. An independent calibration is needed to determine the electrometric response as millivolts per one charge (q) across the membrane. For this purpose, the electron redistribution in the partially reduced MV-CO ("mixed valence" with bound CO) cytochrome oxidase was followed after CO photolysis (for details see [20]). The MV state is formed in the presence of CO under anaerobic conditions. It has the redox centers of the BNC reduced, whereas all other sites are oxidized or partly reduced.

Binding of CO to the reduced BNC increases the redox-potential of heme a_3. Upon the laser pulse, CO is dissociated from heme a_3 resulting in lowering of its redox potential driving redistribution of electrons in the enzyme (reversed electron transfer, or the "back-flow" reaction). Three electron equilibration processes can be resolved in the bovine oxidase at neutral pH. The shortest electron transfer from heme a_3 to heme a occurs in the nanosecond time regime ($\tau \sim 1.2$ ns) [54]. This is followed by a slower electron transfer equilibration between the hemes with $\tau \sim 3$ μs, which is rate-limited by the kinetics of CO dissociation from the Cu_B center [54,55]. The next transition step happens in 30–50 μs and includes electron redistribution from the heme a/heme a_3 pair to Cu_A.

After removing oxygen, caa_3 oxidase was incubated under CO atmosphere and the appearance of the CO-mixed valence enzyme was detected spectroscopically. To assign the microsecond and millisecond phases of absorbance changes following dissociation of CO from the mixed-valence and fully reduced states of caa_3 oxidase, we recorded the surface of optical changes in the wavelength range between 350 and 850 nm with a frequency up to 1 spectrum/μs.

Fig. 2 shows the time course of the reaction upon CO photolysis from the mixed valence state at the characteristic wavelengths extracted from the complete matrix of the collected spectra. The kinetics of absorption changes starts with an unresolved jump, caused mostly by CO dissociation from heme a_3. Subsequent transitions of redox states of the hemes a/a_3 can be traced at 605 nm and 445 nm (Fig. 2). In contrast to the bovine enzyme, where the electron transfer between hemes a_3 and a with $\tau \sim 3$ μs results in a sharp decrease of absorbance at 445 nm with parallel increase at 605 nm, the kinetics of absorption changes of caa_3 oxidase at 445 nm looks similar to those at 605 nm. No traces of an absorbance decrease with a ~3 μs time constant were observed. Meanwhile, transient absorbance changes with $\tau \sim 40$–50 μs can be observed at all the characteristic wavelengths.

Similar to bovine oxidase, the initial jump at 830 nm caused by photolysis of CO is succeeded by an absorbance decrease due to Cu_A reduction with $\tau \sim 40$–50 μs (Fig. 2). In parallel, the absorbance increase at 550 nm reflects electron redistribution to cytochrome c. The yield of the electron transfer to Cu_A and further to cytochrome c, which are in rapid redox equilibrium, depends on the initial state of the enzyme and increases with further reduction of the mixed valence state (Fig. 2, dotted lines). Fig. 3 shows the dependence of the extent of the cytochrome c reduction in the back-flow reaction on redox potential. The redox potential (E_h) was estimated from parallel registration of the redox state of cytochrome c of *T. thermophilus* caa_3, assuming $E_m \sim 218$ mV [42].

The maximal amplitude of the back-flow reaction is observed at $E_h \sim 245$ mV, which corresponds to a mean of 3.6 electrons per enzyme. This value is ~0.6 electrons more reduced as compared to bovine enzyme [20]. The dependence of the yield of the electron backflow on the initial state of the bovine enzyme reflects a decrease of the midpoint redox potential of the binuclear center in response to the anticooperative redox interaction with the reduced heme a [20]. This effect can be more pronounced in caa_3 oxidase due to additional anticooperative interaction with the extra redox-center, cytochrome c.

Fig. 4 shows the result of decomposition of the three-dimensional absorbance-time-wavelength surfaces into kinetic spectral components, upon CO photolysis from two states of enzyme, *viz.* the mixed

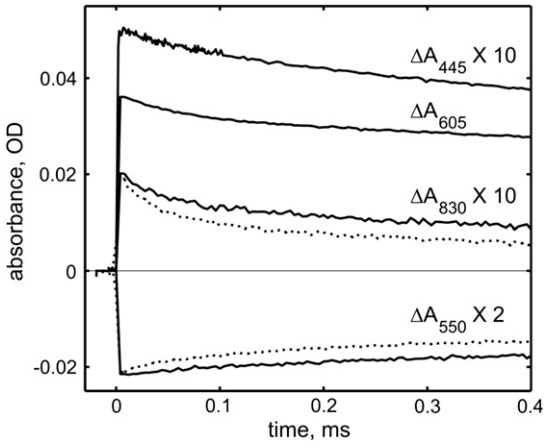

Fig. 2. The kinetics of electron back-flow in caa_3 oxidase monitored by optical spectroscopy at hemes a and a_3 (605 nm), cytochrome c (550 nm, multiplied × 2), Cu_A (830 nm, multiplied × 10), and hemes a and a_3 (445 nm).The kinetic curves were extracted from the absorbance-time-wavelength surface of optical changes after CO dissociation from mixed-valence caa_3 cytochrome oxidase from *T. thermophilus*. Solid lines: data recorded for the mixed-valence state of caa_3 oxidase; dotted lines: the kinetics at 550 nm and 830 nm recorded in case of the maximal extent of the reversed electron transfer to the input redox-centers (Cu_A and cytochrome c), obtained after prolonged incubation with CO and normalized to the corresponding curves by the amplitude of the CO photolysis phase. Conditions: caa_3 cytochrome oxidase, 16.5 μM; CO, 0.2 mM; DM, 0.1%; HEPES (7.5), 200 mM; optical path, 1 cm.

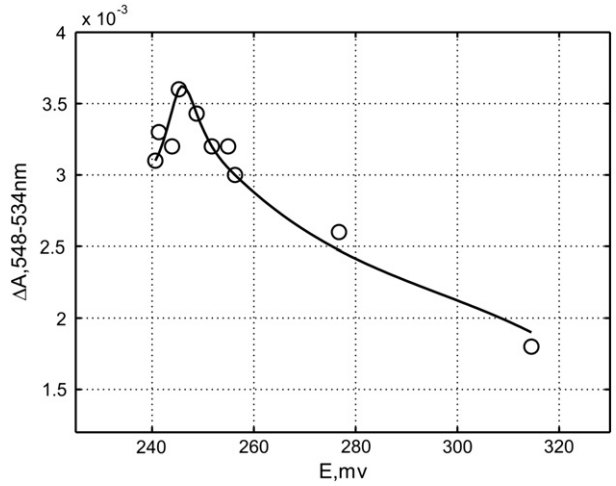

Fig. 3. Dependence of the amplitude of electron back-flow in the 40–60 μs phase of caa_3 oxidase. The apparent redox potential was estimated from the extent of cytochrome *c* reduction (~26% for maximal amplitude of the back-flow reaction), revealed from parallel registration of static spectra and assuming E_m~218 mV for cytochrome *c* of *T. thermophilus* caa_3 [42].

valence state of caa_3 with maximal yield of Cu_A/cytochrome *c* reduction during the backflow reaction (Fig. 4A, B), and the fully reduced state of caa_3 oxidase (Fig. 3C, D), where there is no "backflow". Analysis revealed two spectral components for both states. For the mixed-valence state, the spectrum of the first resolved component (~40 μs) clearly shows a trough near 606 nm and the appearance of a peak at around 550 nm (Fig. 4A). In addition, it is characterized by a charge-transfer band with maximum around 665 nm and a broad decrease of absorption at the near-infrared band of Cu_A (790–830 nm, not shown). This component primarily reflects the electron transfer from the low spin heme *a* and high spin heme a_3 into the input redox-centers, Cu_A and cytochrome *c*.

The second resolved phase is characteristic for CO recombination to the reduced heme a_3. This component exhibits a peak at around 590 nm and a through at 612 nm (Fig. 4B). It reproduces the second resolved component with k_{app}~70 s^{-1} in the fully reduced enzyme (Fig. 4D), in general agreement with literature data [36,53,56]. Apart from the millisecond phase, photolysis of CO from the fully reduced caa_3 oxidase is followed by a spectral transition with τ~30 μs (Fig. 4C). This is close to the time constant of CO dissociation from Cu_B revealed by an FTIR study of caa_3 oxidase from *T. thermophilus* [56]. The spectrum of this component is characterized by a broad peak at ~600 nm and a trough at ~625 nm. These values are in agreement with the spectral shift of heme a_3 (with τ~3 μs) induced by CO release from Cu_B in the fully reduced bovine enzyme [57], provided that the maxima of the heme a_3 redox spectrum in cytochrome caa_3 from *T. thermophilus* are red-shifted compared to that of bovine aa_3. The red-shifted feature of caa_3 from *T. thermophilus* is in agreement with earlier data [36], and may be caused by the replacement of the farnesyl side chain of the heme a_3 in the caa_3 from *T. thermophilus* with geranylgeranyl group [58].

We suggest that the ~3 μs electron re-equilibration step caused by release of CO from Cu_B is about ten times delayed in the caa_3 from *T. thermophilus* relative to the bovine enzyme. Hence, it contributes to the major electron transfer in the back-flow occurring with τ~40 μs. It is noted that the absence of ~3 μs electron transfer in the back-flow reaction has been mentioned earlier for caa_3 enzyme from *Bacillus PS3* [59]. Meanwhile, this phase was demonstrated during a study of caa_3 from *Bacillus stearothermophilus* [51], probably reflecting variability in the properties of the heme–copper oxidases.

Fig. 5 shows modeling of the ~40 μs phase of the back-flow reaction using difference (reduced *minus* oxidized) spectra of heme *a*, heme a_3, cytochrome *c* and the spectral shift of heme a_3, induced by the CO release from Cu_B (Fig. 4C). A reasonable fit for the moment of maximal extent of the back-flow reaction can be achieved assuming that ~0.4 μM of heme *a* and ~0.6 μM of heme a_3 are oxidized during this transition, whereas ~0.2 μM of cytochrome *c* and ~0.8 μM of Cu_A are reduced. The maximal extent of electron transfer from the heme a/a_3 pair to the Cu_A/cytochrome *c* pair can thus be estimated to be 0.10–0.12 electron equivalents per enzyme molecule. This process is expected to involve charge movement across the membrane and can be used for charge transfer calibration.

The ultrafast kinetics of the electron transfer between hemes, observed earlier on the nanosecond time scale [54], is beyond the resolution of our measuring system. Nevertheless, the optical changes of caa_3 during CO photolysis in the submicrosecond time scale can still be extracted by extrapolation of the global fits to the time of the laser flash (Fig. 6A). The obtained spectra are distinct for the fully reduced and mixed-valence states, which indicate unresolved submicrosecond electron equilibration in the mixed-valence state of caa_3 oxidase. The difference between the two spectra is characterized by a peak at 598 nm and a trough at 619 nm (Fig. 6B). It can be well

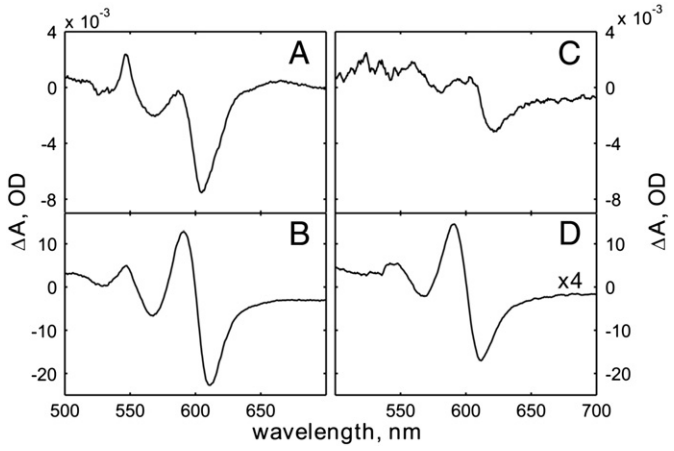

Fig. 4. The spectra of the components in the absorbance-time-wavelength surface of optical changes after CO dissociation from mixed-valence (A, B) and fully reduced (C, D) caa_3 cytochrome oxidase from *T. thermophilus*. A. The first resolved component with τ~39.6 μs upon CO photolysis from the mixed-valence caa_3. B. The second resolved component (τ~0.72 ms). The time constant is shortened due to the short registration time of monitoring. C. The first resolved component with τ~30 μs upon CO photolysis from the fully reduced enzyme. D. The second resolved component (τ~13.5 ms, multiplied by 4).

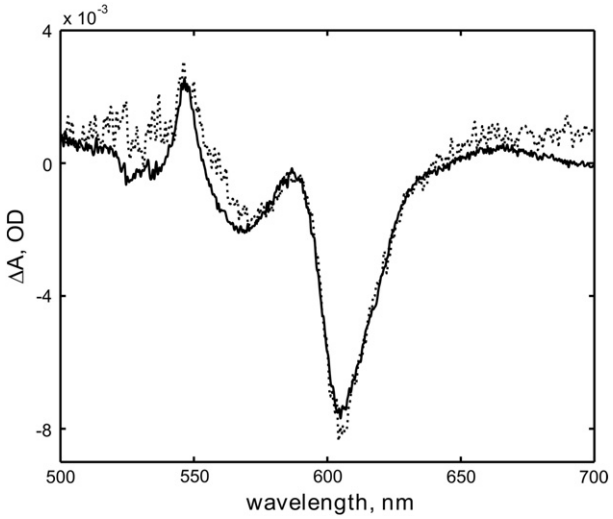

Fig. 5. Modeling of the ~40 μs component of the back-flow electron transfer (solid line), using the basic spectra of reduction of heme *a*, heme a_3, cytochrome *c* and the spectral shift of heme a_3 (dotted line).

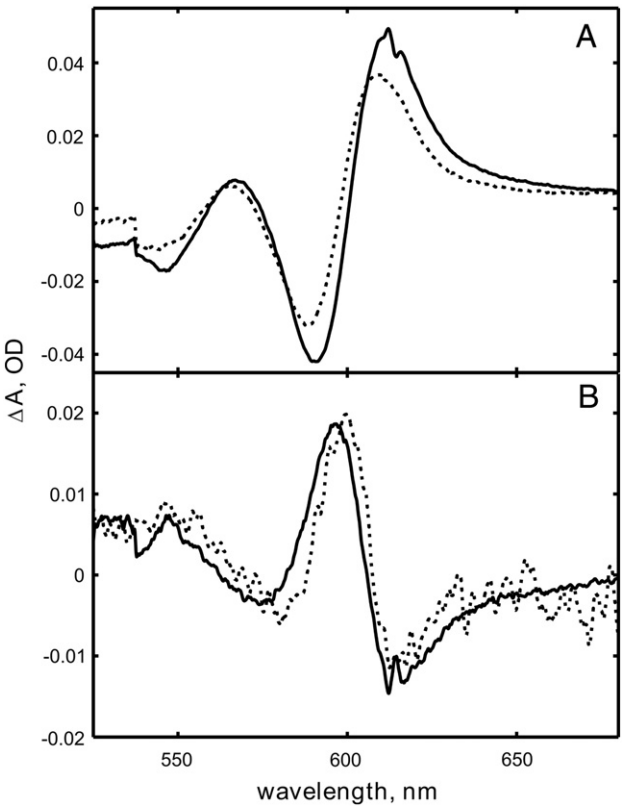

Fig. 6. A. CO photolysis spectra in fully reduced (solid line) and mixed valence (dashed line) states, obtained from extrapolating global fits to the data at $\tau = 0$. B. The difference (mixed-valence *minus* fully reduced) between the two spectra in A (solid line). Modeling of the unresolved back-flow component at the nanosecond time scale, using reduced *minus* oxidized difference spectra of heme *a*, heme a_3, and cytochrome *c* (dotted line).

fitted by using the pure stationary redox spectra of heme a_3 and heme *a* of caa_3 oxidase from *T. thermophilus* [36], taken with equal amplitudes and opposite signs (Fig. 6B, dotted line), and thus corresponds to the equivalent oxidation of heme a_3 and reduction of heme *a* in ~10–15% of the caa_3 enzyme population, which is similar to the bovine enzyme [54].

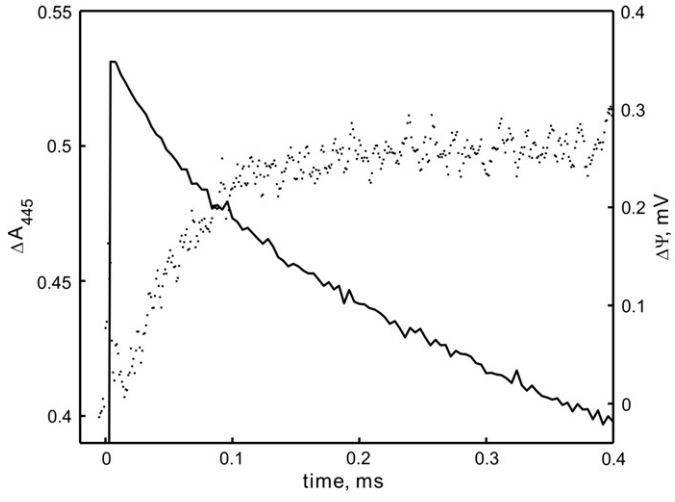

Fig. 7. The kinetics of electron back-flow in caa_3 oxidase monitored by the electrometric measurements (dotted line, right axis) and by the optical changes at the reduced heme a/a_3 band (445 nm, solid line, left axis). Optical measurement and electrometric conditions were as in Figs. 2 and 1, respectively.

3.3. Electrometric measurements of electron "back-flow" in cytochrome caa_3

Fig. 7 shows the parallel kinetics of membrane potential generation, caused by the electron transfer from BNC to the input redox centers during the back-flow electron transfer, monitored by potentiometric electrometry (Fig. 7, dotted line). Just after the flow-flash turnover, the enzyme was incubated in CO atmosphere in the presence of glucose oxidase, which eliminates the traces of oxygen and causes gradual decrease of the redox-potential with parallel formation of the mixed-valence state of the binuclear center. The kinetics of membrane potential generation coupled to the electron "back-flow" contains a major phase with τ ~40–50 μs corresponding to transfer of negative charge through the enzyme toward the P-side of the membrane. In parallel, the optical absorbance changes at 445 nm that correspond to the oxidation of hemes *a* and a_3 are shown (Fig. 7, solid line). One can see that the fast phase of the optical changes (τ ~40–50 μs) essentially coincides with the electrometric curve, whereas the slow component is due to the electrically silent recombination of CO to the reduced heme a_3.

Based on the general similarity of the 3D structures of caa_3 and aa_3 oxidases [38], we assume that electron distribution between cytochrome *c* and Cu_A as well as between hemes *a* and a_3, is not electrogenic [19] and that the dielectric distance between heme a_3/heme *a* and Cu_A may be estimated as 0.32 of the total membrane dielectric. Further, from the maximal amplitude of charge translocation during the 40 μs phase of electron back-flow (0.33 mV), one can estimate the amplitude of the electrogenic phase, corresponding to electron transfer between heme a_3/heme *a* and cytochrome c/Cu_A couples in 100% of the photoactivated caa_3 cytochrome oxidase as 0.33 mV/0.12 = 2.75 mV, where 0.12 is the fraction of oxidase that participates in the electron transfer between the BNC/heme *a* and Cu_A/cytochrome *c* redox couples (see Section 3.2 above). Hence, the amplitude of the electrometric response upon transfer of a single charge across the entire membrane dielectric is 2.75/0.32 = 8.6 mV.

The total amplitude of charge translocation coupled to the reaction of the fully reduced (five electron reduced) caa_3 cytochrome oxidase with oxygen in the same sample was about 51 ± 2 mV, which therefore corresponds to transfer of 51/8.6 or ~5.9 electrical charges across the membrane.

4. Discussion

4.1. Charge transfer steps linked to the oxidation of the fully reduced cytochrome caa_3 by oxygen

4.1.1. The $R \rightarrow A \rightarrow P_R$ transition

The generation of potential by caa_3 oxidase starts with a lag-phase, which involves the electrically silent release of CO and binding of dioxygen with formation of compound **A** [23]. The lag-phase (τ ~25 μs) is much longer than that for the bovine enzyme [20]. Our previous spectroscopic study of cytochrome caa_3 showed on one hand similar rate constants of generation of compound **A** (τ ~7–10 μs) for both enzymes, but on the other, a significantly smaller yield of the **A** state in caa_3 oxidase [36]. The smaller yield of compound **A** has been proposed to be due to the slower rate of CO dissociation from Cu_B – CO [36], which limits the rate of oxygen binding [53]. This is corroborated by the delayed spectral shift of heme a_3 in the fully reduced enzyme (τ ~30 μs, Fig. 4B, dotted line) that can be attributed to release of CO from Cu_B by analogy with the bovine enzyme. As a consequence, the amplitude of **A** is smaller resulting in an apparent delay of the subsequent potential generation steps during formation of the $\mathbf{P_R}$ state, and prolongation of the lag-phase relative to the aa_3 oxidase [20].

The second resolved phase is characterized by a time constant of 25–30 μs, which is very close to that expected for generation of the $\mathbf{P_R}$ state based on the kinetics of optical changes [36]. The amplitude of the 25 μs component varied throughout the fitting of different

traces (1.5–7%), whereas the combined amplitudes of the second and third components remained constant. The low accuracy in determination of the contribution of the second phase is probably attributable to the extended preceding lag-phase.

During the $\mathbf{A}\rightarrow\mathbf{P_R}$ transition, the binuclear center receives an electron from heme *a* and the O–O bond is split with formation of the ferryl form of heme a_3 (Fe^{IV}=O). Taking the maximal amplitude of the $\mathbf{A}\rightarrow\mathbf{P_R}$ transition as 3.77 mV it is possible to estimate the distance of charge translocation as

$$3.77\,\text{mV}\ (\text{amplitude of the phase}) \times \frac{5.9\ (\text{number of transferred charges})}{51\,\text{mV}\ (\text{total amplitude})} = 0.44.$$

This value amounts to translocation of 1 charge across about 12 Å, assuming a 28 Å dielectric thickness of the membrane, which is very close to the value obtained for aa_3-type cytochrome oxidase from *Paracoccus denitrificans*. In the latter case, the $\mathbf{A}\rightarrow\mathbf{P_R}$ transition is coupled to charge transfer across ~11 Å [6], which was suggested to be mainly due to internal proton transfer from Glu-278 (*P. denitrificans* numbering) to a so far unidentified acceptor above the heme groups, the putative proton-loading site (PLS). This proton transfer reaction is proposed to be the initial step of the proton pump mechanism [23]. In addition, breaking of the oxygen-oxygen bond during formation of $\mathbf{P_R}$ requires delivery of a "chemical" proton from the conserved tyrosine residue at the active site [48]. In contrast, during the $\mathbf{A}\rightarrow\mathbf{P_R}$ transition of ba_3 oxidase from *T. thermophilus* [24], this electrogenic event is associated with charge transfer across only ~4 Å [24], which was attributed solely to proton transfer from the conserved tyrosine to help scission of the O–O bond.

In cytochrome caa_3, we suggest that the **A** to $\mathbf{P_R}$ transition includes delivery of a chemical proton from the conserved Tyr-254/His-250 pair to the BNC (~4 Å) and loading of a PLS (~8 Å) by a proton for pumping, similar to the case of the aa_3-type enzyme. If the PLS is located in close proximity of the propionates of heme a_3 [60], and since the gating glutamate (Glu-278) is absent from the A2 type oxidases (such as the caa_3 studied here), the Tyr-248/Ser-249 pair may be the source of the pumped proton (YS-pair in Fig. 8), instead of the glutamate, as proposed [35,38].

4.2. The $P_R\rightarrow F$ transition

The third phase of the electrometric response has the largest relative amplitude and a time constant of about 45 μs, which is close to the rate of the $\mathbf{P_R}\rightarrow\mathbf{F}$ transition detected by the kinetics of optical changes [36]. The $\mathbf{P_R}\rightarrow\mathbf{F}$ transition in the aa_3-type oxidases is coupled to transfer of about 1.3–1.6 charges across the membrane [6,23]. It includes electron redistribution between Cu_A and heme *a* (across ~0.32 of the dielectric), and proton transfer from the N-phase to the vicinity of heme a_3, most likely to the Cu_B bound hydroxyl [24,48,49]. The proton transfer from the N-phase to the Cu_B alters the α-band spectrum of the ferryl compound of heme a_3 (shift of the peak from 607 to 580 nm, [61]) and

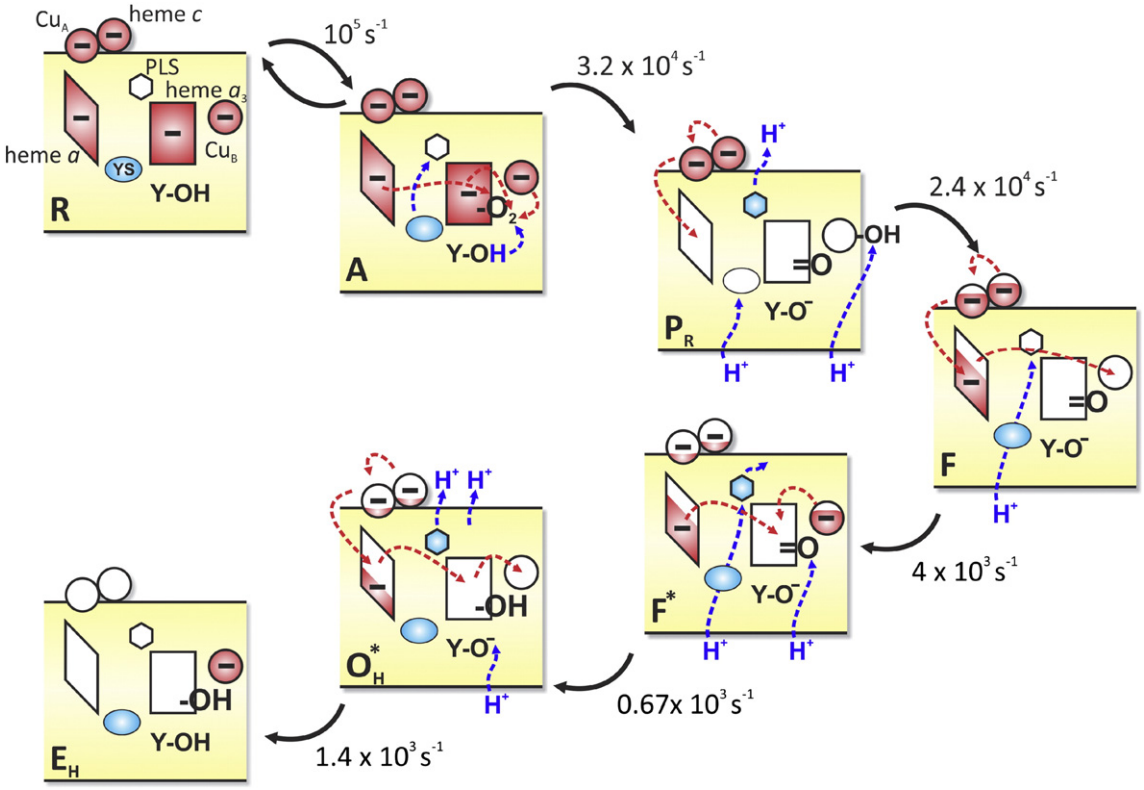

Fig. 8. Reaction scheme: The rhombus and square represent hemes *a* and a_3, respectively. The circles above the hemes represent cytochrome *c* and Cu_A, while the circle next to heme a_3 represents Cu_B. The hexagon represents the proton loading site (PLS). Y-OH represents the conserved Tyr-250 residue in the active site of caa_3 cytochrome oxidase from *T. thermophilus*. The oval represents the proposed internal proton donor, the YS pair (Tyr-248/Ser-249). The filled circles/rhombuses indicate the reduced state of the respective redox center, and the filled hexagon indicates the proton-loading state of the PLS. The partially filled elements correspond to the partial reduction of the corresponding redox centers. The dashed arrows indicate electron and proton transfers during the subsequent reaction step. The reaction of the fully reduced cytochrome caa_3 with dioxygen starts with the binding of O_2 to heme a_3 (compound **A**), which is followed by electron transfer from heme *a* to the BNC, forming the $\mathbf{P_R}$ state. During the $\mathbf{A}\rightarrow\mathbf{P_R}$ transition, the O–O bond is split with formation of the ferryl form of heme a_3 (Fe^{IV}=O). Three out of four electrons required for oxygen reduction at this stage are taken from the BNC, whereas the fourth electron is delivered to dioxygen molecule from the low-spin heme *a* and is accompanied by a delivery of a "chemical" proton from the cross-linked tyrosine (Tyr-250) at the active site. Further, the two electrons, equilibrated among the three input redox-centers, heme *a*, Cu_A and cytochrome *c*, are transferred one by one into the BNC during the reduction of compound **F**, converting the BNC via the $\mathbf{O_H}$ state into the final product of the reaction, the $\mathbf{E_H}$ state where Cu_B is the final electron acceptor. For details of the transient proton transfer steps coupled to the conversion of the corresponding intermediates of enzyme, see the text.

corresponds to the translocation of ~0.68 charge equivalents. The electron redistribution between Cu_A and heme *a* gives a relative electrometric amplitude of: $0.32 \times 0.6 = 0.19$, where 0.6 is the extent of electron transfer from Cu_A in this step [62], and 0.32 is the fraction of the total membrane dielectric crossed by the electron. In addition, the $\mathbf{P_R} \rightarrow \mathbf{F}$ transition in the typical aa_3 oxidases completes the pumping of one proton across the membrane [22], that was initiated during the $\mathbf{A} \rightarrow \mathbf{P_R}$ transition [23]. Namely, this step includes release of the pumped proton from the PLS to the output P-side water phase (~0.15 charge equivalents, [6]) together with reprotonation of the Glu-278 (~0.56 charge equivalents, [4,63]).

The amplitude of the third resolved transition in cytochrome caa_3 from *T. thermophilus* corresponds to translocation of 0.27×5.9 charges = 1.59 charges across the complete span of the membrane dielectric, which clearly shows coupling of this step to pumping of one proton. We suggest that this step includes translocation of a chemical proton to the BNC and electron redistribution between the cytochrome c/Cu_A pair and heme *a*. The latter gives a contribution of: $0.75 * 0.32 = 0.24$, where 0.75 is the extent of electron transfer to heme *a*, derived from the spectroscopic measurements in this step [36]. In addition, the pumped proton is most likely expelled from the PLS together with reprotonation of the Tyr-248/Ser-249 pair (YS, in Fig. 8) from the inner water phase. In summary, this estimate yields $0.67 + 0.24 + 0.15 + 0.56 = 1.63$ charge equivalents for the $\mathbf{P_R} \rightarrow \mathbf{F}$ transition of the caa_3 enzyme. Combined with the $\mathbf{A} \rightarrow \mathbf{P_R}$ transition, the total amplitude of membrane potential generation during the overall $\mathbf{A} \rightarrow \mathbf{P_R} \rightarrow \mathbf{F}$ event of cytochrome caa_3 suggests a total transfer of two charges across the membrane (Fig. 8), which is similar to the case in aa_3-type oxidases [23].

4.3. The electrogenic events coupled to the $\mathbf{F} \rightarrow \mathbf{O_H} \rightarrow \mathbf{E_H}$ transitions

The $\mathbf{F} \rightarrow \mathbf{O}$ transition is the slowest final step during oxygen reduction in the typical aa_3 oxidases, and is driven by transfer of an electron equivalent shared between the low-spin heme *a* and Cu_A to the BNC, and formation of the ferric state of heme a_3 ($\mathbf{O}$) [22,64,65]. Similar to $\mathbf{A} \rightarrow \mathbf{P_R} \rightarrow \mathbf{F}$, the $\mathbf{F} \rightarrow \mathbf{O}$ transition is associated with translocation of two charges through the membrane [16,20,23]. More specifically, this catalytic stage of the typical aa_3 oxidases from *Rhodobacter sphaeroides* and *P. denitrificans* is coupled to translocation of the "pumped" and "chemical" protons, reflected generally by two electrogenic components similar in amplitude with time constants of about 0.2–0.4 ms and 1.4–1.6 ms [6,20–22,46,66,67].

As shown for the aa_3 oxidase from *P. denitrificans*, the 0.2 ms electrogenic step corresponds to translocation of ~1.0 charge equivalents [45]. This includes proton transfer from the immediate donor (Glu-278) to the pump site (PLS) [21,45,68], which is accompanied by simultaneous reprotonation of Glu-278 from the N-phase [46,69] resulting in transfer of approximately ~0.85 charge equivalents through the membrane [6,45]. The second electrogenic component of the resolved $\mathbf{F} \rightarrow \mathbf{O}$ transition (τ ~1.5 ms; ~0.96 charge equivalents [6]) of aa_3 cytochrome oxidase is assigned to two simultaneous processes [7,21,46]. First, release of the pumped proton from the PLS to the P-side of the membrane yields one charge transfer across ~15% of the dielectric barrier [6,45]. Secondly, chemical proton uptake from the inner water phase to the BNC corresponds to proton transfer through ~2/3 of the membrane dielectric. The minor variation between the amplitudes of the electrogenic phases and the corresponding sets of the assigned proton transfer events can be explained by the additional charge transfer due to the electron redistribution from Cu_A to BNC of the remaining 0.4 electron equivalents [62].

In the kinetics of membrane potential generation of the caa_3 cytochrome oxidase from *T. thermophilus* enzyme, the fourth (0.25 ms) and fifth (1.4 ms) electrogenic components demonstrate similar time constants to the $\mathbf{F} \rightarrow \mathbf{O}$ transition of aa_3 oxidases, whereas the additional electrogenic component (τ ~4 ms) is unique and was not observed during a recent flow-flash study of the aa_3 and ba_3 oxidases from *T. thermophilus* [22,24,49,50]. The overall amplitude of these three electrogenic phases of caa_3 cytochrome oxidase is about twice that of the $\mathbf{A} \rightarrow \mathbf{P_R} \rightarrow \mathbf{F}$ transitions, and hence corresponds to electrogenic transfer of a total of four charges across the membrane. That is, if the $\mathbf{F} \rightarrow \mathbf{O_H}$ transition of caa_3 from *T. thermophilus* is coupled to the translocation of two charges, as is the case for aa_3, it follows that the transfer of the fifth electron into the BNC during conversion of the $\mathbf{O_H}$ state into $\mathbf{E_H}$ is linked to translocation of two additional charges. The relative amplitudes of the individual electrogenic components can be calibrated, yielding translocation of ~1.1 (~0.25 ms), ~1.53 (~1.4 ms) and ~1.2 (~4 ms) charge equivalents, respectively.

By analogy with mitochondrial-like aa_3 oxidases, the 0.25 ms component of caa_3 can be attributed to an electrogenic transfer of the pumped proton from the N-side water phase, via the YS pair, to the PLS, located above the binuclear center ($\mathbf{F} \rightarrow \mathbf{F}^*$ transition in the Fig. 8; ~0.85 charge equivalents). This could take place together with additional transfer of the ~0.25 charge equivalents due to electron redistribution from the Cu_A/heme *c* pair to the BNC. Notice that the total extent of Cu_A and cytochrome *c* reduction in the **F** state of caa_3 oxidase from *T. thermophilus* corresponds to about 1.3 electron equivalents [36]. Hence, translocation of this amount of electrons across one-third of the dielectric to BNC would bring in an additional $1.3 * 0.32$, or ~0.43 translocated charge equivalents.

The amplitude of the 1.4 ms electrogenic phase in caa_3 corresponds to translocation of ~1.53 charge equivalents. As found by optical spectroscopy, the decay of the **F** state in a single-turnover of caa_3 takes place in the course of several milliseconds, and is associated with transfer of two electrons into the BNC, converting the binuclear center to the one-electron reduced $\mathbf{E_H}$ state ($\mathbf{F} \rightarrow \mathbf{O_H} \rightarrow \mathbf{E_H}$ transitions) [36]. We suggest that the 1.4 ms electrogenic phase reflects the overall uptake of two protons ($\mathbf{F}^* \rightarrow \mathbf{O_H}^*$ in Fig. 8), including transfer of a substrate proton linked to generation of the $\mathbf{O_H}$ state (across ~2/3 of the dielectric barrier) and, additionally, uptake of the second pumped proton into the PLS (~0.85 charge equivalents).

The amplitude of the third electrogenic component (~4 ms) is equal to translocation of ~1.2 charge equivalents, which may include uptake of the chemical proton into the BNC needed for the $\mathbf{O_H} \rightarrow \mathbf{E_H}$ transition (~2/3 of the dielectric barrier), plus release of the 2 pumped protons to the P-site of the membrane (~0.3 charge equivalents). In addition, this component may include the resting electrogenic electron transfer (~0.2 charge equivalents) from the input redox centers to the BNC ($\mathbf{O_H}^* \rightarrow \mathbf{E_H}$ transition, Fig. 8). In accord with [70,71], full oxidation of Cu_A may be needed to gate the release of the pumped proton. As a result, both of the pumped protons, which are associated with $\mathbf{F} \rightarrow \mathbf{O_H}$ and $\mathbf{O_H} \rightarrow \mathbf{E_H}$ transitions, respectively, may be expelled to the P-phase during the ~4 ms phase.

In summary, we suggest that the electrogenic transfer of electrons to the BNC during $\mathbf{F} \rightarrow \mathbf{O_H} \rightarrow \mathbf{E_H}$ happens during the ~0.25 ms and ~4 ms phases, since their relative amplitudes are larger in comparison with the assigned protonic steps. In the spectroscopic study of the caa_3, the $\mathbf{F} \rightarrow \mathbf{O_H} \rightarrow \mathbf{E_H}$ sequence was detected as a single optical transition with τ ~2.5 ms [36]; the absence of a separate 0.25 ms phase may be explained if electron transfer during the $\mathbf{F} \rightarrow \mathbf{F}^*$ transition proceeds mostly from Cu_A to Cu_B, which does not produce significant changes of absorption.

As suggested for aa_3 oxidase, the highly hydrophilic domain above the hemes through which release of the pumped protons takes place could also be able to store protons, possibly delaying their exit to the P-side of the membrane [72]. Thus we may propose that the slow (4 ms) uptake of the chemical proton, linked to the $\mathbf{O_H} \rightarrow \mathbf{E_H}$ transition is rate-limited by the release of a pumped proton through the exit path. It should be mentioned that ~4 ms component is in reasonable agreement with recently reported steady-state turnover of caa_3 from *T. thermophilus* (185 s^{-1}, [73]).

As we have shown recently, about half of the enzyme molecules do not contain CO on the heme a_3 and is non-photoreactive in the flow-flash study due to peculiarities of ligand binding to the BNC of the caa_3 oxidase [36]. As a result, the unphotolyzed oxidation by oxygen of the non-photoreactive part of enzyme may lead to the relatively slow (from hundred milliseconds up to seconds) electron re-equilibration within the cytochrome caa_3 with the significant admixture of the reduced heme *a* in the final state of enzyme [36,74]. At the same time, the photolyzed, active in ligand binding part of caa_3 oxidase, which was actually tested during this work, is oxidized in a short time to the final E_H state with location of 5-th electron in a binuclear center (but not on a heme *a*), and the reduction of BNC by the 5-th electron is coupled to the pumping of a proton.

In conclusion, the electrogenic components associated with the $\mathbf{A \rightarrow P_R \rightarrow F}$ transitions in the kinetics of membrane potential generation coupled to oxidation of the fully reduced cytochrome caa_3 from *T. thermophilus* reflect transfer of approximately two charges through the membrane, similarly to the typical aa_3 oxidases. The subsequent three electrogenic phases associated with the $\mathbf{F \rightarrow O_H \rightarrow E_H}$ transitions correspond to translocation of another 4 charges. Assuming that the $\mathbf{F \rightarrow O_H}$ transition of caa_3 from *T. thermophilus* is coupled to the translocation of two charges, as is the case for aa_3, it follows that the transfer of the additional electron into the BNC during conversion of the $\mathbf{O_H}$ state into $\mathbf{E_H}$ is linked to translocation of two charges. In the past, the $\mathbf{O_H \rightarrow E_H}$ transition was shown to be coupled to proton translocation in the conventional aa_3-type oxidases by artificial electron injection into the oxidized enzyme (see Introduction), but only if the enzyme had been oxidized by O_2 just before light-activation of the redox dye. Here, by the use of the five-electron-reduced cytochrome caa_3 from *T. thermophilus*, we have confirmed this notion using the additional electron present naturally in the fully reduced enzyme.

Acknowledgements

This work was supported by the Russian Foundation for Basic Research (to S.A.S., grants 09-04-00140 and 12-04-01000), Biocentrum Helsinki, Sigrid Jusélius Foundation, the Academy of Finland (to M.I.V., I. B., M.W.), and the Science Foundation of Ireland BICF685 (to T.S.).

References

[1] S. Ferguson-Miller, G.T. Babcock, Heme/copper terminal oxidases, Chem. Rev. 7 (1996) 2889–2907.
[2] I. Belevich, M.I. Verkhovsky, Molecular mechanism of proton translocation by cytochrome *c* oxidase, Antioxid. Redox Signal. 10 (2008) 1–29.
[3] P. Brzezinski, J. Reimann, P. Adelroth, Molecular architecture of the proton diode of cytochrome *c* oxidase, Biochem. Soc. Trans. 36 (2008) 1169–1174.
[4] S.A. Siletsky, J. Zhu, R.B. Gennis, A.A. Konstantinov, Partial steps of charge translocation in the nonpumping N139L mutant of *Rhodobacter sphaeroides* cytochrome *c* oxidase with a blocked D-Channel, Biochemistry 49 (2010) 3060–3073.
[5] J. Koepke, E. Olkhova, H. Angerer, H. Muller, G. Peng, H. Michel, High resolution crystal structure of *Paracoccus denitrificans* cytochrome *c* oxidase: new insights into the active site and the proton transfer pathways, Biochim. Biophys. Acta 1787 (2009) 635–645.
[6] I. Belevich, E. Gorbikova, N.P. Belevich, V. Rauhamaki, M. Wikstrom, M.I. Verkhovsky, Initiation of the proton pump of cytochrome *c* oxidase, Proc. Natl. Acad. Sci. U. S. A. 107 (2010) 18469–18474.
[7] S.A. Siletsky, A.A. Konstantinov, Cytochrome *c* oxidase: charge translocation coupled to single-electron partial steps of the catalytic cycle, Biochim. Biophys. Acta 1817 (2012) 476–488.
[8] P. Mitchell, Chemiosmotic Coupling and Energy Transduction, Glynn Research Ltd., Bodmin, 1968.
[9] M.K. Wikström, Proton pump coupled to cytochrome *c* oxidase in mitochondria, Nature 266 (1977) 271–273.
[10] S. Iwata, C. Ostermeier, B. Ludwig, H. Michel, Structure at 2.8 Å resolution of cytochrome *c* oxidase from *Paracoccus denitrificans*, Nature 376 (1995) 660–669.
[11] S. Yoshikawa, K. Shinzawa-Itoh, R. Nakashima, R. Yaono, E. Yamashita, N. Inoue, M. Yao, M.J. Fei, C.P. Libeu, T. Mizushima, H. Yamaguchi, T. Tomizaki, T. Tsukihara, Redox-coupled crystal structural changes in bovine heart cytochrome *c* oxidase, Science 280 (1998) 1723–1729.
[12] T. Soulimane, G. Buse, G.P. Bourenkov, H.D. Bartunik, R. Huber, M.E. Than, Structure and mechanism of the aberrant ba_3-cytochrome *c* oxidase from *Thermus thermophilus*, EMBO J. 19 (2000) 1766–1776.
[13] M. Svensson-Ek, J. Abramson, G. Larsson, S. Tornroth, P. Brzezinski, S. Iwata, The X-ray crystal structures of wild-type and EQ(I-286) mutant cytochrome *c* oxidases from *Rhodobacter sphaeroides*, J. Mol. Biol. 321 (2002) 329–339.
[14] M.I. Verkhovsky, A. Jasaitis, M.L. Verkhovskaya, J.E. Morgan, M. Wikstrom, Proton translocation by cytochrome *c* oxidase, Nature 400 (1999) 480–483.
[15] D. Bloch, I. Belevich, A. Jasaitis, C. Ribacka, A. Puustinen, M.I. Verkhovsky, M. Wikström, The catalytic cycle of cytochrome *c* oxidase is not the sum of its two halves, Proc. Natl. Acad. Sci. U. S. A. 101 (2004) 529–533.
[16] S. Siletsky, A.D. Kaulen, A.A. Konstantinov, Resolution of electrogenic steps coupled to conversion of cytochrome *c* oxidase from the peroxy to the ferryl-oxo state, Biochemistry 38 (1999) 4853–4861.
[17] Q.H. Gibson, C. Greenwood, Reactions of cytochrome oxidase with oxygen and carbon monoxide, Biochem. J. 86 (1963) 541–554.
[18] D. Zaslavsky, A.D. Kaulen, I.A. Smirnova, T. Vygodina, A.A. Konstantinov, Flash-induced membrane potential generation by cytochrome *c* oxidase, FEBS Lett. 336 (1993) 389–393.
[19] D.L. Zaslavsky, I.A. Smirnova, S.A. Siletsky, A.D. Kaulen, F. Millett, A.A. Konstantinov, Rapid kinetics of membrane potential generation by cytochrome *c* oxidase with the photoactive Ru(II)-tris-bipyridyl derivative of cytochrome *c* as electron donor, FEBS Lett. 359 (1995) 27–30.
[20] A. Jasaitis, M.I. Verkhovsky, J.E. Morgan, M.L. Verkhovskaya, M. Wikström, Assignment and charge translocation stoichiometries of the major electrogenic phases in the reaction of cytochrome *c* oxidase with dioxygen, Biochemistry 38 (1999) 2697–2706.
[21] S.A. Siletsky, A.S. Pawate, K. Weiss, R.B. Gennis, A.A. Konstantinov, Transmembrane charge separation during the ferryl-oxo→oxidized transition in a nonpumping mutant of cytochrome *c* oxidase, J. Biol. Chem. 279 (2004) 52558–52565.
[22] C. Ribacka, M.I. Verkhovsky, I. Belevich, D.A. Bloch, A. Puustinen, M. Wikström, An elementary reaction step of the proton pump is revealed by mutation of tryptophan-164 to phenylalanine in cytochrome *c* oxidase from *Paracoccus denitrificans*, Biochemistry 44 (2005) 16502–16512.
[23] I. Belevich, M.I. Verkhovsky, M. Wikstrom, Proton-coupled electron transfer drives the proton pump of cytochrome *c* oxidase, Nature 440 (2006) 829–832.
[24] S.A. Siletsky, I. Belevich, A. Jasaitis, A.A. Konstantinov, M. Wikström, T. Soulimane, M.I. Verkhovsky, Time-resolved single-turnover of ba_3 oxidase from *Thermus thermophilus*, Biochim. Biophys. Acta 1767 (2007) 1383–1392.
[25] A.J. Moody, 'As prepared' forms of fully oxidised haem/Cu terminal oxidases, Biochim. Biophys. Acta 1276 (1996) 6–20.
[26] P. Adelroth, R.B. Gennis, P. Brzezinski, Role of the pathway through K(I-362) in proton transfer in cytochrome *c* oxidase from *R. sphaeroides*, Biochemistry 37 (1998) 2470–2476.
[27] N. Capitanio, T.V. Vygodina, G. Capitanio, A.A. Konstantinov, P. Nicholls, S. Papa, Redox-linked protolytic reactions in soluble cytochrome *c* oxidase from beef-heart mitochondria: redox Bohr effects, Biochim. Biophys. Acta 1318 (1997) 255–265.
[28] S.E. Brand, S. Rajagukguk, K. Ganesan, L. Geren, M. Fabian, D. Han, R.B. Gennis, B. Durham, F. Millett, A new ruthenium complex to study single-electron reduction of the pulsed O_H state of detergent-solubilized cytochrome oxidase, Biochemistry 46 (2007) 14610–14618.
[29] S.A. Siletsky, I. Belevich, M. Wikström, T. Soulimane, M.I. Verkhovsky, Time-resolved $O_H \rightarrow E_H$ transition of the aberrant ba_3 oxidase from *Thermus thermophilus*, Biochim. Biophys. Acta 1787 (2009) 201–205.
[30] M.I. Verkhovsky, A. Tuukkanen, C. Backgren, A. Puustinen, M. Wikstrom, Charge translocation coupled to electron injection into oxidized cytochrome *c* oxidase from *Paracoccus denitrificans*, Biochemistry 40 (2001) 7077–7083.
[31] D. Jancura, V. Berka, M. Antalik, J. Bagelova, R.B. Gennis, G. Palmer, M. Fabian, Spectral and kinetic equivalence of oxidized cytochrome *c* oxidase as isolated and "activated" by reoxidation, J. Biol. Chem. 281 (2006) 30319–30325.
[32] J.A. Fee, M.G. Choc, K.L. Findling, R. Lorence, T. Yoshida, Properties of a copper-containing cytochrome c_1aa_3 complex: a terminal oxidase of the extreme thermophile *Thermus thermophilus* HB8, Proc. Natl. Acad. Sci. U. S. A. 77 (1980) 147–151.
[33] T. Yoshida, J.A. Fee, Studies on cytochrome *c* oxidase activity of the cytochrome c_1aa_3 complex from *Thermus thermophilus*, J. Biol. Chem. 259 (1984) 1031–1036.
[34] K. Hon-nami, T. Oshima, Purification and characterisation of cytochrome *c* oxidase from *Thermus thermophilus* HB8, Biochemistry 23 (1984) 454–460.
[35] M.M. Pereira, M. Santana, M. Teixeira, A novel scenario for the evolution of haem–copper oxygen reductases, Biochim. Biophys. Acta 1505 (2001) 185–208.
[36] S.A. Siletsky, I. Belevich, N.P. Belevich, T. Soulimane, M.I. Verkhovsky, Time-resolved single-turnover of caa_3 oxidase from *Thermus thermophilus*. Fifth electron of the fully reduced enzyme converts O_H into E_H state, Biochim. Biophys. Acta 1807 (2011) 1162–1169.
[37] S. Siletskiy, T. Soulimane, N. Azarkina, T.V. Vygodina, G. Buse, A. Kaulen, A. Konstantinov, Time-resolved generation of a membrane potential by ba_3 cytochrome *c* oxidase from *Thermus thermophilus*. Evidence for reduction-induced opening of the binuclear center, FEBS Lett. 457 (1999) 98–102.
[38] J.A. Lyons, D. Aragao, O. Slattery, T. Soulimane, M. Caffrey, Structural insights into electron transfer in caa_3-type cytochrome oxidase, Nature 487 (2012) 514–518.
[39] B.C. Hill, C. Greenwood, Spectroscopic evidence for the participation of compound A (Fea_3^{2+}–O_2) in the reaction of mixed-valence cytochrome *c* oxidase with oxygen at room temperature, Biochem. J. 215 (1983) 659–667.
[40] M.I. Verkhovsky, J.E. Morgan, M. Wikström, Oxygen binding and activation: early steps in the reaction of oxygen with cytochrome *c* oxidase, Biochemistry 33 (1994) 3079–3086.
[41] S. Gerscher, P. Hildebrandt, T. Soulimane, G. Buse, Resonance Raman spectroscopic study of the caa_3 oxidase from *Thermus thermophilus*, Biospectroscopy 4 (1998) 365–377.

[42] P. Hellwig, T. Soulimane, W. Mantele, Electrochemical, FT-IR and UV/VIS spectroscopic properties of the *caa*$_3$ oxidase from *T. thermophilus*, Eur. J. Biochem. 269 (2002) 4830–4838.
[43] C.M. Gomes, C. Backgren, M. Teixeira, A. Puustinen, M.L. Verkhovskaya, M. Wikstrom, M.I. Verkhovsky, Heme–copper oxidases with modified D- and K-pathways are yet efficient proton pumps, FEBS Lett. 497 (2001) 159–164.
[44] D.A. Bloch, A. Jasaitis, M.I. Verkhovsky, Elevated proton leak of the intermediate O_H in cytochrome *c* oxidase, Biophys. J. 96 (2009) 4733–4742.
[45] I. Belevich, D.A. Bloch, N. Belevich, M. Wikström, M.I. Verkhovsky, Exploring the proton pump mechanism of cytochrome *c* oxidase in real time, Proc. Natl. Acad. Sci. U. S. A. 104 (2007) 2685–2690.
[46] S.A. Siletsky, D. Han, S. Brand, J.E. Morgan, M. Fabian, L. Geren, F. Millett, B. Durham, A.A. Konstantinov, R.B. Gennis, Single-electron photoreduction of the P_M intermediate of cytochrome *c* oxidase, Biochim. Biophys. Acta 1757 (2006) 1122–1132.
[47] L.A. Drachev, A.A. Jasaitis, A.D. Kaulen, A.A. Kondrashin, E.A. Liberman, I.B. Nemecek, S.A. Ostroumov, A.Y. Semenov, V.P. Skulachev, Direct measurement of electric current generation by cytochrome oxidase, H^+-ATPase and bacteriorhodopsin, Nature 249 (1974) 321–324.
[48] E.A. Gorbikova, I. Belevich, M. Wikström, M.I. Verkhovsky, The proton donor for O–O bond scission by cytochrome *c* oxidase, Proc. Natl. Acad. Sci. U. S. A. 105 (2008) 10733–10737.
[49] A. Jasaitis, C. Backgren, J.E. Morgan, A. Puustinen, M.I. Verkhovsky, M. Wikström, Electron and proton transfer in the arginine-54-methionine mutant of cytochrome *c* oxidase from *Paracoccus denitrificans*, Biochemistry 40 (2001) 5269–5274.
[50] H. Lepp, E. Svahn, K. Faxen, P. Brzezinski, Charge transfer in the K proton pathway linked to electron transfer to the catalytic site in cytochrome *c* oxidase, Biochemistry 47 (2008) 4929–4935.
[51] A. Giuffre, E. D'Itri, S. Giannini, M. Brunori, T. Ubbink-Kok, W.N. Konings, G. Antonini, The *caa*$_3$ terminal oxidase of *Bacillus stearothermophilus*. Transient spectroscopy of electron transfer and ligand binding, J. Biol. Chem. 271 (1996) 13987–13992.
[52] B.C. Hill, Stopped-flow, laser-flash photolysis studies on the reactions of CO and O_2 with the cytochrome *caa*$_3$ complex from *Bacillus subtilis*: conservation of electron transfer pathways from cytochrome *c* to O_2, Biochemistry 35 (1996) 6136–6143.
[53] W.H. Woodruff, Coordination dynamics of heme–copper oxidases. The ligand shuttle and the control and coupling of electron transfer and proton translocation, J. Bioenerg. Biomembr. 25 (1993) 177–188.
[54] E. Pilet, A. Jasaitis, U. Liebl, M.H. Vos, Electron transfer between hemes in mammalian cytochrome *c* oxidase, Proc. Natl. Acad. Sci. U. S. A. 101 (2004) 16198–16203.
[55] M.I. Verkhovsky, A. Jasaitis, M. Wikstrom, Ultrafast haem–haem electron transfer in cytochrome *c* oxidase, Biochim. Biophys. Acta 1506 (2001) 143–146.
[56] E. Pinakoulaki, T. Soulimane, C. Varotsis, Fourier transform infrared (FTIR) and step-scan time-resolved FTIR spectroscopies reveal a unique active site in cytochrome *caa*$_3$ oxidase from *Thermus thermophilus*, J. Biol. Chem. 277 (2002) 32867–32874.
[57] O. Einarsdottir, R.B. Dyer, D.D. Lemon, P.M. Killough, S.M. Hubig, S.J. Atherton, J.J. Lopez-Garriga, G. Palmer, W.H. Woodruff, Photodissociation and recombination of carbonmonoxy cytochrome oxidase: dynamics from picoseconds to kiloseconds, Biochemistry 32 (1993) 12013–12024.
[58] M. Lubben, K. Morand, Novel prenylated hemes as cofactors of cytochrome oxidases. Archaea have modified hemes A and O, J. Biol. Chem. 269 (1994) 21473–21479.
[59] S. Hirota, M. Svensson-Ek, P. Adelroth, N. Sone, T. Nilsson, B.G. Malmström, P. Brzezinski, A flash-photolysis study of the reactions of a *caa*$_3$-type cytochrome oxidase with dioxygen and carbon monoxide, J. Bioenerg. Biomembr. 28 (1996) 495–501.
[60] V.R. Kaila, V. Sharma, M. Wikstrom, The identity of the transient proton loading site of the proton-pumping mechanism of cytochrome c oxidase, Biochim. Biophys. Acta 1807 (2011) 80–84.
[61] M. Wikstrom, Active site intermediates in the reduction of O_2 by cytochrome oxidase, and their derivatives, Biochim. Biophys. Acta 1817 (2012) 468–475.
[62] B.C. Hill, The reaction of the electrostatic cytochrome *c*-cytochrome oxidase complex with oxygen, J. Biol. Chem. 266 (1991) 2219–2226.
[63] D.M. Medvedev, E.S. Medvedev, A.I. Kotelnikov, A.A. Stuchebrukhov, Analysis of the kinetics of the membrane potential generated by cytochrome *c* oxidase upon single electron injection, Biochim. Biophys. Acta 1710 (2005) 47–56.
[64] M. Oliveberg, P. Brzezinski, B.G. Malmström, The effect of pH and temperature on the reaction of fully reduced and mixed-valence cytochrome *c* oxidase with dioxygen, Biochim. Biophys. Acta 977 (1989) 322–328.
[65] B.C. Hill, C. Greenwood, The reaction of fully reduced cytochrome *c* oxidase with oxygen studied by flow-flash spectrophotometry at room temperature, Biochem. J. 218 (1984) 913–921.
[66] S.A. Siletsky, A.D. Kaulen, D. Mitchell, R.B. Gennis, A.A. Konstantinov, in: EBEC Short Reports, Resolution of two proton conduction pathways in cytochrome *c* oxidase, 9, 1996, p. 90.
[67] A.A. Konstantinov, S. Siletsky, D. Mitchell, A. Kaulen, R.B. Gennis, The roles of the two proton input channels in cytochrome c oxidase from *Rhodobacter sphaeroides* probed by the effects of site-directed mutations on time resolved electrogenic intraprotein proton transfer, Proc. Natl. Acad. Sci. U. S. A. 94 (1997) 9085–9090.
[68] M. Wikstrom, M.I. Verkhovsky, G. Hummer, Water-gated mechanism of proton translocation by cytochrome *c* oxidase, Biochim. Biophys. Acta 1604 (2003) 61–65.
[69] M.I. Verkhovsky, I. Belevich, D.A. Bloch, M. Wikstrom, Elementary steps of proton translocation in the catalytic cycle of cytochrome oxidase, Biochim. Biophys. Acta 1757 (2006) 401–407.
[70] M.A. Sharpe, S. Ferguson-Miller, A chemically explicit model for the mechanism of proton pumping in heme–copper oxidases, J. Bioenerg. Biomembr. 40 (2008) 541–549.
[71] K. Kirchberg, H. Michel, U. Alexiev, Net proton uptake is preceded by multiple proton transfer steps upon electron injection into cytochrome *c* oxidase, J. Biol. Chem. 287 (2012) 8187–8193.
[72] L. Salomonsson, K. Faxen, P. Adelroth, P. Brzezinski, The timing of proton migration in membrane-reconstituted cytochrome *c* oxidase, Proc. Natl. Acad. Sci. U. S. A. 102 (2005) 17624–17629.
[73] T. Soulimane, M. von Walter, P. Hof, M.E. Than, R. Huber, G. Buse, Cytochrome-*c*552 from *Thermus thermophilus*: a functional and crystallographic investigation, Biochem. Biophys. Res. Commun. 237 (1997) 572–576.
[74] H. Sigurdson, A. Namslauer, M.M. Pereira, M. Teixeira, P. Brzezinski, Ligand binding and the catalytic reaction of cytochrome *caa*$_3$ from the thermophilic bacterium *Rhodothermus marinus*, Biochemistry 40 (2001) 10578–10585.